Clinical and Translational Radiation Oncology 51 (2025) 100916

Contents lists available at ScienceDirect

Clinical and Translational Radiation Oncology

journal homepage: www.sciencedirect.com/journal/clinical-and-translational-radiation-oncology

Impact of tumor position displacement during end-exhalation breath-hold condition on tumor dose in lung stereotactic body radiation therapy using volumetric modulated arc therapy

Tatsuya Kamima [a,b,*], Shunsuke Moriya [b], Takeji Sakae [b], Hikaru Miyauchi [a], Yasushi Ito [a], Kenji Tokumasu [a], Yasuo Yoshioka [a]

[a] Radiation Oncology Department, Cancer Institute Hospital, Japanese Foundation for Cancer Research, 3-8-31 Ariake, Koto-ku, Tokyo 135-8550, Japan
[b] Faculty of Medicine, University of Tsukuba, 1-1-1, Tennodai, Tsukuba, Ibaraki 305-8575, Japan

ARTICLE INFO

Keywords:
Stereotactic body radiation therapy
End-exhalation breath-holding
Cine CT
Volumetric modulated arc therapy
4D dose calculation

ABSTRACT

Background and purpose: In lung stereotactic body radiation therapy (SBRT) using a breath-holding technique, displacement of tumor during breath-holding is rarely considered. This study used four-dimensional (4D) dose calculation with cine computed tomography (CT) to evaluate the impact of unexpected tumor position displacement during breath-holding on the target dose of lung volumetric modulated arc therapy (VMAT)-SBRT.
Materials and methods: This study included 20 cases for which tumor position displacement during end-exhalation breath-holding (range: 0.5–12.6 mm) was evaluated on cine CT. VMAT-SBRT plans (3D dose) were generated using treatment planning CT images (reference CT) acquired during end-exhalation breath-hold. For each plan, the 4D dose was calculated using deformable image registration of the cine CT images and was accumulated onto the reference CT. Dose metrics and the mean biologically effective dose at $\alpha/\beta = 10$ (BED_{10}) for the gross tumor volume (GTV) were compared between 3D and 4D doses.
Results: In the 17 cases where the tumor was within the planning target volume (PTV) during breath-holding, the difference between the 3D and 4D doses was within 3 % for each dose metric. However, in 3 cases where the tumor position during breath-holding included displacement outside the PTV, both the $D_{98\%}$ and mean BED_{10} of the GTV were reduced by 6.9–20.0 % and 2.1–13.8 %, respectively, in 4D doses compared to 3D doses.
Conclusion: Our study showed that tumor position displacements during breath-holding may lead to substantial tumor dose reduction.

Introduction

Stereotactic body radiation therapy (SBRT) is established as a primary treatment option for early-stage non-small cell lung cancer and solitary lung metastases because it has demonstrated a 90 % local control (LC) rate, which is comparable to that of surgery [1–5]. To achieve the necessary treatment accuracy for hypofractionated high doses, it is imperative to precisely localize and immobilize the targeted tumor during treatment. Several respiratory motion management methods have been proposed to reduce intrafractional variability, among which the breath-holding technique is a major one for lung SBRT because it reduces the irradiated volume without invasiveness [6–11].

The breath-holding technique should take into account not only the variability in tumor position between breath-holding periods and within one treatment fraction, but also the tumor motion during one breath-holding period. In this regard, a recent study used cine computed

Abbreviations: SBRT, Stereotactic body radiation therapy; LC, local control; CT, computed tomography; 4D, four-dimensional; VMAT, volumetric modulated arc therapy; FFF, flattening filter-free; MLC, multileaf collimator; DIR, deformable image registration; RPM, real-time position management; HU, Hounsfield units; GTV, gross tumor volume; ITV, internal target volume; PTV, planning target volume; JCOG, Japan Clinical Oncology Group; SDG, small displacement group; MDG, medium displacement group; LDG, large displacement group; DVF, deformation vector field; DSC, Dice similarity coefficient; MDA, mean distance to agreement; HI, homogeneity index; BED, biologically effective dose.

* Corresponding author at: Radiation Oncology Department, Cancer Institute Hospital, Japanese Foundation for Cancer Research, 3-8-31 Ariake, Koto-ku, Tokyo 135-8550, Japan.
E-mail address: tatsuya.kamima@jfcr.or.jp (T. Kamima).

https://doi.org/10.1016/j.ctro.2025.100916
Received 1 September 2024; Received in revised form 31 October 2024; Accepted 6 January 2025
Available online 8 January 2025

tomography (CT) to evaluate the four-dimensional (4D) motion of lung tumors during end-exhalation breath-holding [12]. During breath-holding, tumors were assumed to be static in the lungs; however, in some cases their position drifted both gradually and substantially during end-exhalation breath-holding. Such displacement of the tumor position during breath-holding is not yet widely described. Furthermore, in clinical practice, tumor dynamics during breath-holding are rarely evaluated for each patient. If treatment planning does not take into account tumor displacement during breath-holding, there is concern that the tumor may be subject to displacement outside of the target volume during irradiation.

Four-dimensional dose calculation is a method to simulate dose variations in a moving tumor during irradiation. Previous reports on 4D dose calculations focused mostly on dosimetric evaluation of tumors moving within the target volume [13–16], and there are no reports evaluating the variations in tumor dose when tumor is displaced outside of the target volume during irradiation. Therefore, dose variations when the tumor position is displaced outside of the target volume during breath-hold irradiation cannot be estimated from previous studies of 4D dose calculations.

For SBRT treatments, volumetric modulated arc therapy (VMAT) is used in combination with flattening filter-free (FFF) beams. For hypofractionated high dose VMAT, interplay effects between the multileaf collimator (MLC) leaf sequence and lung tumor motion might create undesirable hot or cold dose spots inside the target. Previous reports of interplay effects have focused mainly on tumor motion during free breathing [13–16], and many of them concluded that there were no clinically significant effects because they were averaged out over multiple breathing cycles or treatment sessions. Furthermore, in the breath-holding technique, the tumor is static and the interplay effect is negligible. However, there have been no studies of interplay effects on tumors that shift gradually during breath-holding. Furthermore, the number of breath-holds required during irradiation is far less than the number of breaths during free breathing, and it is not clear whether dose variations average out under this situation.

Many studies have used deformable image registration (DIR) applied to 4DCT to investigate the impact of tumor motion on calculation of the 4D dose accumulation [13–19]. In this study, we used cine CT acquired during breath-holding for our 4D dose calculation method. Our primary objective was to use 4D dose calculation to investigate the impact of unexpected displacement of tumor position during breath-holding on the target dose of lung VMAT-SBRT. A secondary objective was to investigate the interplay effect of tumor position displacement during breath-holding.

Materials and methods

Patients

This study retrospectively enrolled 20 patients who received lung SBRT at our institution between April 2020 and March 2022. All patients underwent a cine CT scan during CT simulation. Written informed consent was obtained from all the patients, and our institutional ethics committee approved this study (review board number: 2022-GB-002).

Image acquisition

The CT sequences used in this study were acquired using a 320-row multislice CT scanner (Aquilion ONE/GENESIS Edition; Canon Medical Systems, Otawara, Japan). First, the patients received respiratory coaching before CT scan to train for 15–20 s of voluntary end-exhalation breath-holding without visual feedback. The respiratory signals of each patient were monitored using a real-time position management (RPM) system (Varian Medical Systems, Palo Alto, CA, USA), with the gating window set to ± 1.5 mm around the end-exhalation level.

Second, all patients underwent a helical CT scan during breath-holding (reference CT) to calculate 3D dose distributions. The reference CT scans were acquired with a 2.0-mm slice thickness and 2.0-mm reconstruction interval.

Finally, cine CT was performed to acquire 21 s of continuous data (1.5-s scan time interval) during breath-holding. This cine CT was obtained for one breath-holding period in the volume mode (the superior–inferior coverage was 16 cm/rotation) with neither patient couch movement nor RPM gating. The scan conditions were 120 kV, 200 mA, and 0.275 s during a single rotation. The scan was initiated after confirming that the respiratory waveform was within the ± 1.5 mm gating window. A total of 15 phases of CT volumes were obtained by scanning at 1.5-s time intervals during 21 s of breath-holding. Phases in which the respiratory waveform was beyond the gating window because of unsustained breath-holding were excluded from the evaluation. The cine CT acquired during breath-holding had a 3.0-mm slice thickness and 3.0-mm reconstruction interval [12].

Target delineation

The acquired reference CT and cine CT imaging data were exported to an Eclipse treatment planning system (Ver 16.1; Varian Medical Systems). Targets were manually delineated by a radiation oncologist on the reference CT image, and by a medical physicist on each phase of the cine CT image, using a lung window setting with a window width of 1320 Hounsfield units (HU) and window level of − 360 HU. This lung window setting was a preset value in the Eclipse system, and thus allowed the radiation oncologist and medical physicist to delineate the tumor under the same conditions for all patients. Previous reports showed that similar lung window settings (window width of 1350 HU and window level of − 550 HU) allowed assessment of pulmonary nodule size with high accuracy [20]. Tumor motion during end-exhalation breath-holding was measured by comparing the maximum displacement of the gross tumor volume (GTV) centroid in each phase with its position at the start of end-exhalation breath-holding.

No margin was added to the GTV for the clinical target volume in the reference CT. The internal target volume (ITV) was created by a 3-mm expansion of the GTV. This ITV margin was set to compensate for uncertainty in tumor position reproducibility between breath-holds and variations due to heartbeat [21]. The planning target volume (PTV) was created by adding an isotropic margin of 3 mm to the ITV to account for uncertainties in patient setup and mechanical inaccuracies. These margin sizes were those used at our institution in clinical practice. In this study, fixed margins were applied, assuming that the displacement of the tumor position during breath-holding was not considered in the treatment planning.

Treatment planning

All plans were created according to the Japan Clinical Oncology Group (JCOG) 1408 protocol, which was based on a clinical trial of lung SBRT [22]. Supplementary Table S1 shows the dose constraints for the JCOG 1408 protocol. These plans were created on the reference CT using the Eclipse treatment planning system for the TrueBeam linear accelerator with a Millennium 120-leaf MLC (Varian Medical Systems). The beam parameters were 6 MV FFF coplanar VMAT with a maximum dose rate of 1400 MU/minute. Two partial arcs (right side: 20°–181°, left side: 340°–179°) with collimator angles of 20° and 340° were used. For dose calculation, the Acuros XB algorithm (Varian Medical Systems) was used, with a dose calculation grid size of 1.25 mm. The prescribed dose was 55 Gy in four fractions with the dose covering 95 % of the volume ($D_{95\%}$) of the PTV. The dose distribution of the original plan calculated with the reference CT in the manner so described was defined as the '3D dose'. Table 1 shows clinical data and plan characteristics for each patient. Supplementary Fig. S1 shows the tumor displacements over time during end-exhalation breath-holding in each patient. In this study, the cases were classified into three groups according to the magnitude of

Table 1
Patient characteristics and plan details.

Case	Group	Loc.	Diagnosis	GTV volume [cc]	Absolute maximum displacement of the tumor position during BH LR/AP/SI/3D vector [mm]	Beam-on time Arc1/Arc2 [s]	BH time [s]	Number of BH Arc1/Arc2
1	SDG	RLL	Primary	2.2	0.4/ 0.4/ 0.2/ 0.5	80.2/83.5	21.0	4/4
2		RUL	Primary	1.8	0.5/ 0.5/ 0.3/ 0.7	106.6/108.6	21.0	5/5
3		RUL	Primary	1.1	0.6/ 0.7/ 0.1/ 0.9	110.5/119.0	12.0	9/9
4		RLL	Metastasis	5.5	0.3/ 0.7/ 0.9/ 0.9	81.4/81.9	21.0	4/4
5		RLL	Primary	6.3	0.3/ 0.7/ 0.9/ 1.0	120.3/107.6	21.0	6/5
6		RLL	Primary	1.0	0.7/ 1.0/ 1.2/ 1.3	95.0/96.9	21.0	5/5
7		LLL	Primary	1.7	0.9/ 0.4/ 1.0/ 1.3	74.0/73.4	16.5	5/5
8		RML	Metastasis	8.9	0.6/ 1.1/ 0.8/ 1.4	102.0/105.3	21.0	4/5
9		LUL	Primary	3.5	0.3/ 0.5/ 1.3/ 1.4	104.9/96.8	21.0	5/5
10		RUL	Metastasis	7.2	0.8/ 1.6/ 0.2/ 1.7	121.0/124.3	15.0	8/8
11		LUL	Primary	2.6	0.6/ 1.8/ 1.1 1.9	94.2/97.8	21.0	5/5
12		RLL	Primary	0.4	0.2/ 1.5/ 1.3/ 2.0	111.8/109.8	12.0	9/9
13		RLL	Primary	1.6	0.2/ 0.5/ 2.3/ 2.3	85.0/86.4	21.0	4/4
14		LLL	Metastasis	7.7	1.5/ 1.8/ 1.7/ 2.6	85.0/96.3	19.5	5/5
15	MDG	LLL	Metastasis	11.1	2.4/ 2.1/ 0.6/ 3.2	102.9/104.4	21.0	5/5
16		LLL	Primary	21.0	2.6/ 2.6/ 2.1/ 4.2	81.0/77.1	21.0	4/4
17		RLL	Primary	16.0	2.6/ 2.6/ 2.2/ 4.2	85.2/90.0	21.0	4/5
18	LDG	LLL	Primary	2.4	1.9/ 1.0/ 7.2/ 7.5	90.3/88.7	15.0	6/6
19		RLL	Primary	5.0	4.0/ 6.6/ 0.7/ 7.7	84.8/89.7	21.0	4/5
20		LLL	Primary	0.7	2.4/ 12.0/ 3.1/ 12.6	79.0/94.6	18.0	5/5

Abbreviations: SDG: small displacement group, MDG: medium displacement group, LDG: large displacement group, RUL: Right upper lobe, LUL: Left upper lobe, RML: Right middle lobe, RLL: Right lower lobe, LLL: Left lower lobe, GTV: Gross tumor volume: LR, Left–right; AP, Anterior–posterior; SI, Superior–inferior, BH: Breath-holding.

displacement of the tumor position during breath-holding: a small displacement group (SDG) with displacement < 3 mm; a medium displacement group (MDG) with displacement of 3–6 mm; and a large displacement group (LDG) with displacement ≥ 6 mm.

4D dose calculation

To evaluate the dosimetric impact of displacement due to tumor drift during breath-holding, DIR-based 4D dose accumulation was performed. The schema for this is represented in Fig. 1. The 4D dose calculation steps were as follows. (a) The VMAT-SBRT plan, created for the reference CT, was divided into a total of 158 sub-arc fields (79 sub-arc fields:1 arc), each covering 2.5°. These sub-arc fields were created using the verification plan function in the Eclipse. (b) The delivery time for each sub-arc field was determined from the original plan. (c) The sub-arc fields corresponded to each cine CT phase, and the dose was calculated. The cine CT images acquired during one breath-holding period were used repeatedly for the 4D calculations. This is because the

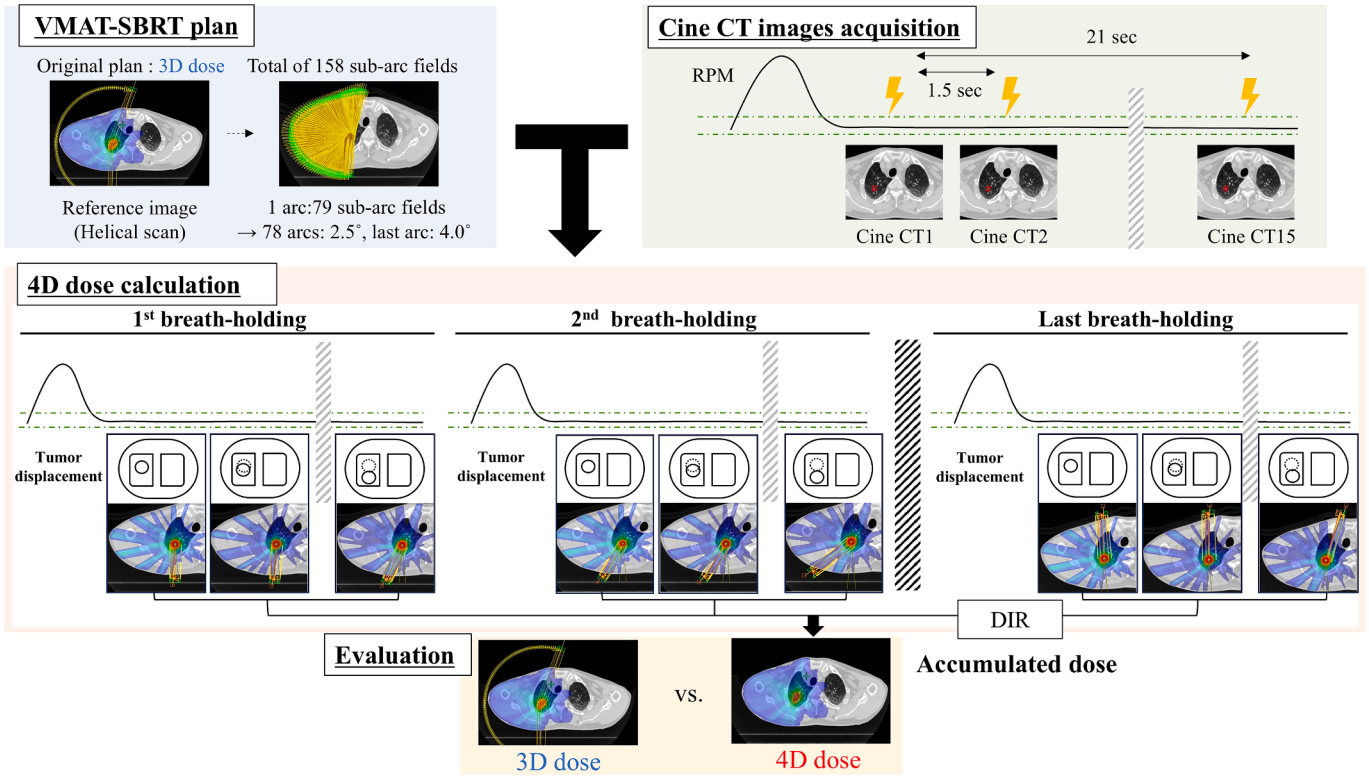

Fig. 1. Overall schema of the four-dimensional dose calculation process. RPM: real-time position management, DIR: deformable image registration, BH: breath-holding.

reproducibility of the displacement of the tumor position during breath-holding is reported to be very high [12]. The uncertainty of inter-breath-holding reproducibility was not considered. (d) To accumulate the dose distributions for each cine CT phase onto the reference CT, DIR was performed using RayStation Ver 10.A (Research Laboratories AB, Stockholm, Sweden). RayStation uses the ANAtomically CONstrained Deformation Algorithm based on free form deformation as the hybrid DIR algorithm [23,24]. To obtain the accumulated dose to the GTV between different CT images, a correspondence between the images is necessary. The DIR was performed with the GTV structure as the focus region, and deformation vector fields (DVFs) were generated. (e) The DVFs were used to warp the dose distribution of the cine CT phase onto the reference CT, and this accumulated total dose distribution included the effect of tumor displacement. The Dice similarity coefficient (DSC) and mean distance to agreement (MDA) of the GTV were employed for quantitative assessment of the DIR. We considered a DSC > 0.8 and MDA < 2 mm to be acceptable values for the accuracy of the DIR, as recommended by the American Association of Physicists in Medicine Task Group publication No 132 [25].

Dosimetric evaluation

To evaluate the impact of the displacement of tumor position during breath-holding on the GTV, the dose distributions from 3D and 4D dose calculations were compared. The $D_{98\%}$, D_{mean}, $D_{2\%}$, and homogeneity index (HI) of the GTV were also analyzed for both methods. D_X is the dose in Gy received by at least X% of the volume. HI was calculated as follows:

$$HI = \frac{D_{2\%} - D_{98\%}}{D_{mean}} \bullet 100[\%] \quad (1)$$

where lower HI values indicate a more homogeneous target dose. The differences in dose metrics between the 3D dose and 4D dose were calculated as follows:

$$\delta = \frac{Metric_{4Ddose} - Metric_{3Ddose}}{Metric_{3Ddose}} \bullet 100[\%] \quad (2)$$

Several investigations have reported that LC in SBRT for lung tumor is associated with the mean biologically effective dose at $\alpha/\beta = 10$ (BED_{10}) for the GTV [26–28]. Therefore, in the present study, D_{mean} was converted to BED_{10} as follows:

$$BED_{10} = 4 \bullet D_{mean}\left(1 + \frac{D_{mean}}{\alpha/\beta}\right) \quad (3)$$

where α/β was set to 10 Gy. The mean BED_{10} for the GTV were compared between the 3D and 4D dose.

Results

Validation of the DIR

Table 2 shows the DSC and MDA of the GTV between the reference CT and each of the deformed cine CTs. In all cases, DSC was > 0.8 and MDA < 2 mm, indicating that the accuracy of the DIR was very high.

Comparison of the 3D and 4D doses in the GTV

Fig. 2 shows the dose difference between the 3D dose distribution and 4D accumulated dose distribution in the reference image for three groups. The LDG showed a substantial dose difference in the direction of the displacement of the tumor. In case 20, which had the largest displacement of tumor position, an underdose was found within the GTV. Conversely, neither hot nor cold dose spots in the dose distribution, which are indicative of interplay effects, were observed in any case.

The median differences in GTV dose metrics between 3D and 4D doses for all cases were as follows: $D_{98\%}$, −0.4 % (range: −20.0 %–2.2 %); D_{mean}, −0.4 % (range: −8.7 %–1.4 %); $D_{2\%}$, −0.1 % (range: −2.2 %–1.1 %); and HI, 0.0 % (range: −2.0 %–19.2 %). Fig. 3 shows a comparison of GTV dose metrics between 3D and 4D doses for each case. In the SDG, the dose difference between the 3D and 4D doses was within 3 % for each dose metric. Furthermore, even in MDG, where the tumor position included displacement outside the ITV during breath-holding, the dose difference between the 3D and 4D doses was within 3 %. Conversely, in LDG, where the tumor position included displacement outside the PTV during breath-holding, the GTV dose was substantially reduced at $D_{98\%}$ (Fig. 3 (a)).

Table 2
The DSC and MDA in each case.

Case #	Group	DSC mean ± SD	MDA [mm] mean ± SD
1	SDG	0.96 ± 0.00	0.14 ± 0.00
2		0.94 ± 0.00	0.18 ± 0.00
3		0.95 ± 0.00	0.12 ± 0.00
4		0.97 ± 0.00	0.10 ± 0.00
5		0.98 ± 0.00	0.08 ± 0.00
6		0.95 ± 0.01	0.20 ± 0.01
7		0.96 ± 0.00	0.11 ± 0.00
8		0.98 ± 0.00	0.08 ± 0.00
9		0.96 ± 0.00	0.14 ± 0.00
10		0.98 ± 0.00	0.10 ± 0.00
11		0.96 ± 0.00	0.10 ± 0.00
12		0.92 ± 0.01	0.24 ± 0.00
13		0.97 ± 0.00	0.08 ± 0.00
14		0.98 ± 0.00	0.09 ± 0.00
15	MDG	0.98 ± 0.00	0.14 ± 0.00
16		0.98 ± 0.00	0.11 ± 0.00
17		0.98 ± 0.00	0.11 ± 0.00
18	LDG	0.97 ± 0.00	0.08 ± 0.00
19		0.98 ± 0.00	0.08 ± 0.00
20		0.93 ± 0.01	0.20 ± 0.01

Abbreviations: SDG: small displacement group, MDG: medium displacement group, LDG: large displacement group, DSC: Dice similarity coefficient, MDA: Mean distance to agreement.

Table 3 shows a comparison of mean BED_{10} between 3D and 4D doses for the GTV in each case. In the SDG and MDG, the differences in mean BED_{10} between 3D and 4D doses were within 3 %, whereas in LDG, the mean BED_{10} was up to 13.8 % lower with the 4D dose compared to the 3D dose.

Discussion

A recent study used cine CT to evaluate the 4D motion of lung tumors during end-exhalation breath-holding and found substantial displacement from the reference position due to tumor drift in several cases [12]. Generally, in SBRT under free breathing, tumor motion is assessed by 4DCT and is considered to be within the target margin as the ITV. However, patient-specific displacement of tumor position during breath-holding is not yet commonly assessed before treatment, and is rarely considered when setting the target margin. This study investigated the impact of displacement of the tumor position during breath-holding on the target dose when isotropic margins (ITV = 3 mm, ITV to PTV = 3 mm) were employed, using a 4D dose calculation with cine CT images. When the tumor position included displacement outside the PTV, as in LDG, the $D_{98\%}$ decreased by 6.9–20.0 % with the 4D calculation. This indicates the need to detect displacement of the tumor position during breath-holding for each patient. Since tumor position displacements such as these do not generally correlate with surrogate markers, such as external marker blocks or the diaphragm, and they are difficult to detect [12], they may result in an unexpected reduction in the dose to the tumor.

From another perspective, Fig. 3 shows that even if large displacement of the tumor of more than 3 mm occurs during breath-holding, as

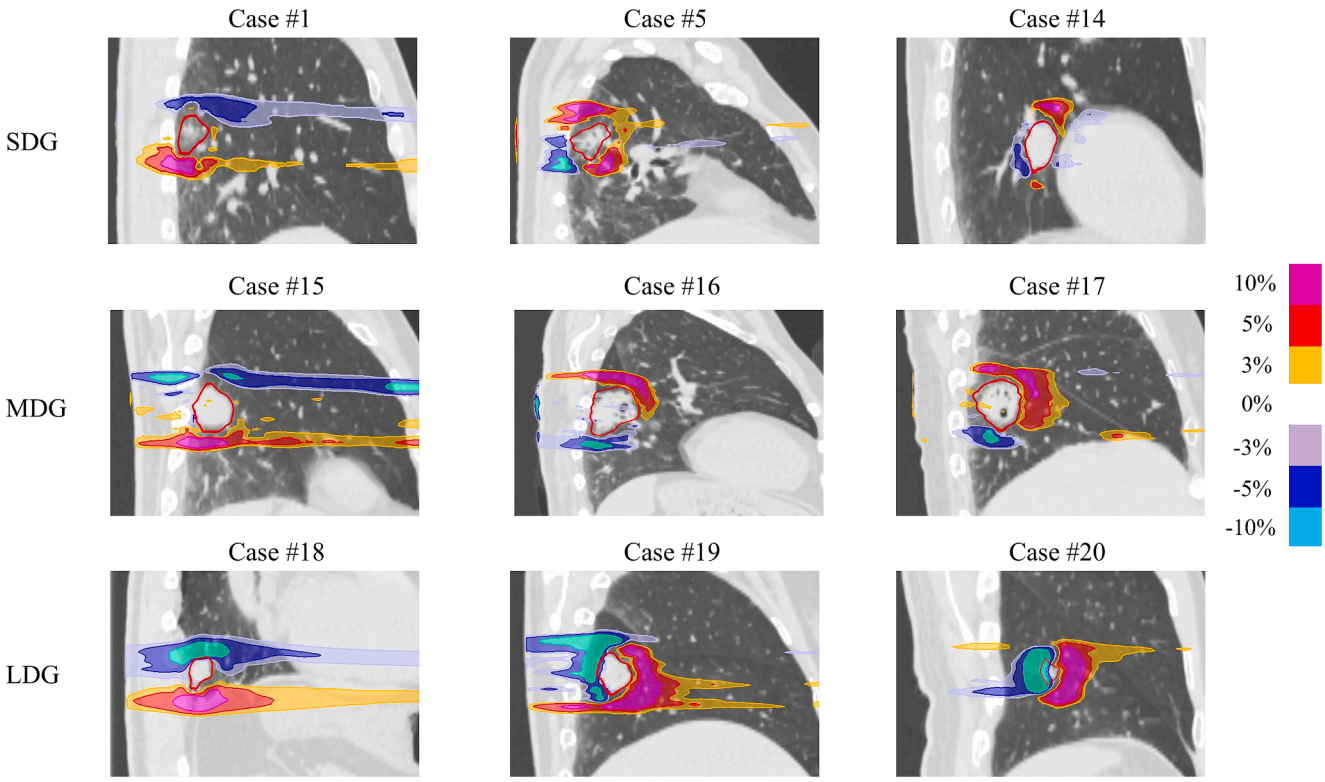

Fig. 2. Dose difference between the 3D dose distribution and 4D accumulated dose distribution in the reference image. SDG extracts representative cases (#1, #5, and #14). The gross tumor volume is represented in thick red. SDG: small displacement group, MDG: medium displacement group, LDG: large displacement group.

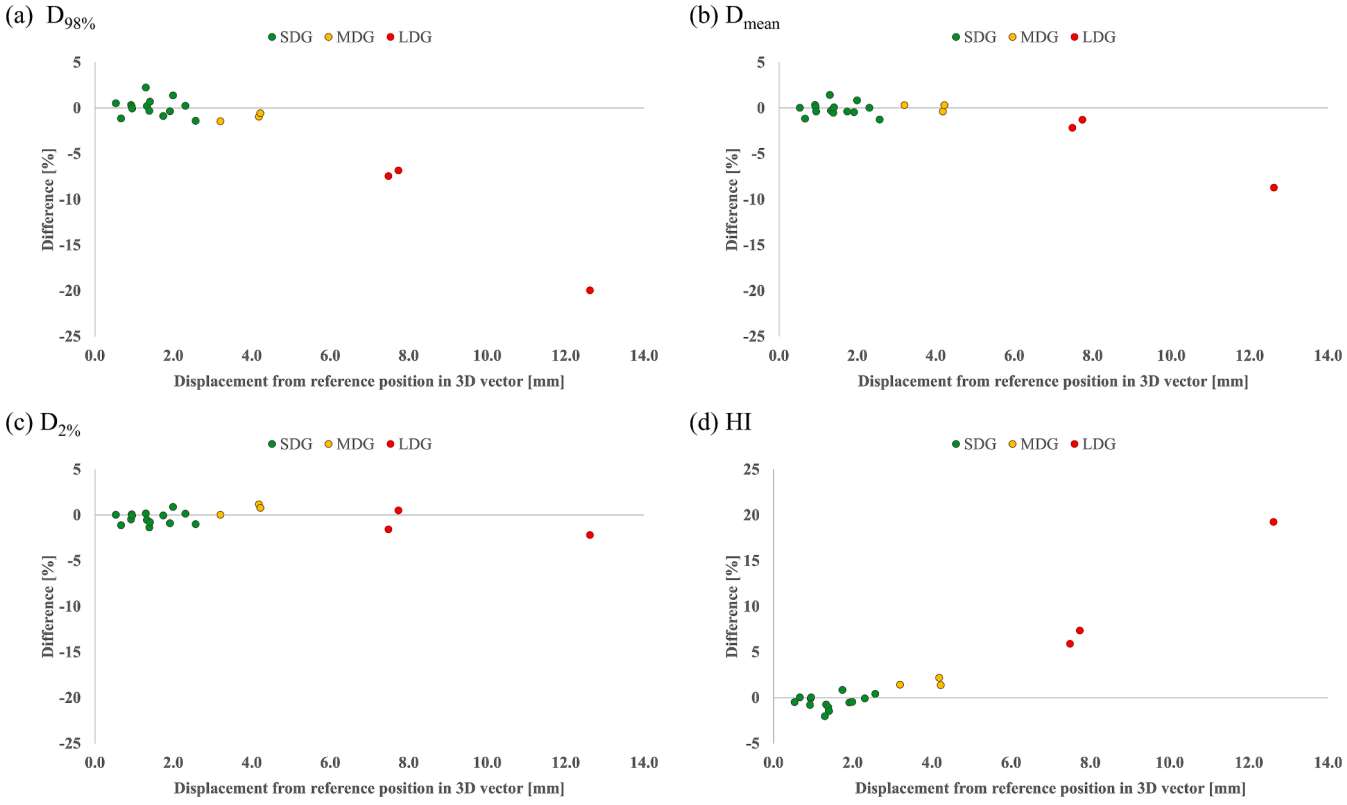

Fig. 3. Comparisons of (a) $D_{98\%}$, (b) D_{mean}, (c) $D_{2\%}$, and (d) HI of the gross tumor volume between 3D and 4D doses for each case. Dx: The minimum dose delivered to x% of the structure volume, HI: homogeneity index, SDG: small displacement group, MDG: medium displacement group, LDG: large displacement group.

Table 3
Mean BED_{10} for the GTV of 3D and 4D doses for each case.

Case #	Group	D_{mean} BED_{10} 3D dose [Gy]	4D dose [Gy]	Difference [%]
1	SDG	183.4	183.4	0.0
2		187.3	183.7	−1.9
3		190.0	191.0	0.5
4		189.5	189.8	0.1
5		184.1	182.9	−0.6
6		184.6	188.9	2.3
7		186.6	185.7	−0.5
8		191.6	189.9	−0.9
9		187.7	187.8	0.1
10		188.9	187.6	−0.7
11		186.7	185.3	−0.8
12		184.0	186.4	1.3
13		183.8	183.8	0.0
14		188.0	184.1	−2.1
15	MDG	192.5	193.5	0.5
16		179.4	178.2	−0.7
17		180.7	181.5	0.5
18	LDG	182.4	175.9	−3.5
19		181.8	178.0	−2.1
20		191.4	165.0	−13.8

Abbreviations: SDG: small displacement group, MDG: medium displacement group, LDG: large displacement group, BED: biologically effective dose.

in the MDG, the dose difference is within 3 % if the tumor is encompassed within the PTV. This result is similar to several reports of 4D dose calculation for SBRT of dynamic lung tumors [13,15,16]. In VMAT-SBRT for lung cancer, treatment planning typically uses fluence optimization of the PTV, and because a significant fraction of this PTV contains low-density lung tissue, more fluences are delivered to increase the dose in the low-density tissue surrounding the tumor [29]. Therefore, we consider that the GTV dose was sufficiently maintained, despite the displacement of the tumor position during breath-holding.

To the best of our knowledge, this is the first study to investigate the interplay effect on tumor position displacement during breath-holding. The impact of the interplay effect on the GTV dose in this study was small (Figs. 2 and 3). In several studies of VMAT-SBRT under free breathing, a large interplay effect was associated with large tumor motion amplitudes, longer breathing periods, and a decreased number of breaths during irradiation [30–32]. In this study, the maximum tumor motion was 12.6 mm. Furthermore, considering one breath-holding period as one breathing period, the maximum duration was 21 s. Stambaugh et al. reported that for simulations, the interplay effect is negligible for 20–30 mm of tumor motion, except for unrealistically long breathing periods (60 s) [33], findings that are in line with the results of the present study. Kubo et al. stated that in actual measurements using a dynamic phantom, the dose error due to interplay effect was averaged out by performing more than 40 breaths during the irradiation of two partial VMAT-SBRT arcs [32]. In contrast, considering the number of breaths as the number of breath-holdings, the maximum number of breath-holdings required for treatment in this calculation method was 18 in case 3 and case 12 (Table 1), which may be assumed to be insufficient to average out the dose errors. However, in this study it did not cause any unexpected dose differences. The interplay effect is a complex phenomenon affected by many factors, including dose fractionation, dose rate, MLC motion complexity, and breathing motion characteristics. Under the conditions of this study, there was no interplay effect due to tumor position displacement during breath-holding.

With lung SBRT, the most unacceptable consequence of the unexpected dose reduction is a reduced LC rate. Table 3 indicates that the mean BED_{10} for the GTV may be decreased by up to 13.8 % if displacement of the tumor position during breath-holding is not taken into account. We note that this error may be overestimated in case No. 20 because the GTV volume is smaller than that of the other cases (see Table 1). Moreover, the mean BED_{10} reduction in the other cases was at most 3.5 %, so the clinical impact would be minimal. However, the 4D dose calculations performed in this study did not include uncertainty in inter-breath-holding reproducibility, which occurs during realistic treatment. A study that evaluated the reproducibility of tumor position between breath holds reported that it is subject to systematic and random geometric uncertainties of approximately 2 mm in each direction [6]. If such uncertainties were taken into account in this study, the tumor doses resulting from the 4D dose calculations could have been further affected. Some studies investigating the association between tumor dose and LC reported that the mean BED_{10} of the GTV requires more than 147–162 Gy [26–28]. However, the optimal prescription dose remains unclear and inconclusive. Moreover, current lung SBRT trends show an increase in the use of low BED regimens over time [34]. With such a treatment strategy, a decrease in the actual tumor dose may affect the clinical outcome. We therefore recommend pretreatment assessment of tumor motion during breath-holding when breath-holding is employed for respiratory motion management.

Previous studies have shown high reproducibility in the displacement of tumor position between breath-holding evaluated on different days [12]. This means that similar motions are likely to occur between multiple breath-holdings. For such highly reproducible motions, it would be possible to compensate by creating a margin for the direction of tumor displacement during breath-holding using the cine CT images acquired during treatment planning. However, few institutions would be able to perform the cine CT used for evaluation in this study because it requires a 320-row multislice CT. An alternative to cine CT for assessing tumor position displacement during breath-holding is to perform multiple go and return imaging with helical scanning. This method would allow evaluation of tumor dynamics during breath-holding at any institution.

Our study has one limitation. The cine CT in this study was acquired with one breath-holding period and the images were used repeatedly for 4D calculations. This means that with multiple breath-holdings being required for a treatment session, there may be variations in the magnitude of displacement of tumor position between different breath-holdings, a factor that was not simulated in this study. However, since the reproducibility of the displacement of tumor position during end-exhalation breath-holding was shown to be high [12], we consider the effects of such variations to be small.

Conclusions

We used 4D calculations with cine CT to evaluate the impact of tumor position displacement during breath-holding on the tumor dose. For tumor position displacements encompassed by the PTV, the dose difference was less than 3 %. Moreover, there was no interplay effect due to tumor position displacement during breath-holding. However, in a case where the tumor position included displacement outside of the PTV during breath-holding, the $D_{98\%}$ was decreased by 6.9–20.0 % and the mean BED_{10} for the GTV by 2.1–13.8 % in comparison with the 3D calculation. Therefore, we recommend that treatment strategies take into account tumor motion during breath-holding.

Funding statement

This study was funded by an institutional research budget of the Japanese Foundation for Cancer Research.

Declaration of competing interest

The authors declare that they have no known competing financial interests or personal relationships that could have appeared to influence the work reported in this paper.

Acknowledgment

We thank Edanz (https://jp.edanz.com/ac) for editing a draft of this manuscript.

Appendix A. Supplementary data

Supplementary data to this article can be found online at https://doi.org/10.1016/j.ctro.2025.100916.

References

[1] Baumann P, Nyman J, Hoyer M, Wennberg B, Gagliardi G, Lax I, et al. Outcome in a prospective phase II trial of medically inoperable stage I non-small-cell lung cancer patients treated with stereotactic body radiotherapy. J Clin Oncol 2009;27:3290–6. https://doi.org/10.1200/JCO.2008.21.5681.

[2] Ogawa Y, Shibamoto Y, Hashizume C, Kondo T, Iwata H, Tomita N, et al. Repeat stereotactic body radiotherapy (SBRT) for local recurrence of non-small cell lung cancer and lung metastasis after first SBRT. Radiat Oncol 2018;13:136. https://doi.org/10.1186/s13014-018-1080-4.

[3] Fakiris AJ, McGarry RC, Yiannoutsos CT, Papiez L, Williams M, Henderson MA, et al. Stereotactic body radiation therapy for early-stage non-small-cell lung carcinoma: four-year results of a prospective phase II study. Int J Radiat Oncol Biol Phys 2009;75:677–82. https://doi.org/10.1016/j.ijrobp.2008.11.042.

[4] De Ruysscher D, Faivre-Finn C, Moeller D, Nestle U, Hurkmans CW, Le Péchoux C, et al. European Organization for Research and Treatment of Cancer (EORTC) recommendations for planning and delivery of high-dose, high precision radiotherapy for lung cancer. Radiother Oncol 2017;124:1–10. https://doi.org/10.1016/j.radonc.2017.06.003.

[5] Zheng X, Schipper M, Kidwell K, Lin J, Reddy R, Ren Y, et al. Survival outcome after stereotactic body radiation therapy and surgery for stage I non-small cell lung cancer: a meta-analysis. Int J Radiat Oncol Biol Phys 2014;90:603–11. https://doi.org/10.1016/j.ijrobp.2014.05.055.

[6] Kimura T, Murakami Y, Kenjo M, Kaneyasu Y, Wadasaki K, Ito K, et al. Interbreath-hold reproducibility of lung tumour position and reduction of the internal target volume using a voluntary breath-hold method with spirometer during stereotactic radiotherapy for lung tumours. Br J Radiol 2007;80:355–61. https://doi.org/10.1259/bjr/31008031.

[7] Kaestner L, Abo-Madyan Y, Huber L, Spaniol M, Siebenlist K, Sacks MK, et al. Motion management in a patient with tracheostomy during lung stereotactic body radiation therapy: breath hold is worth a try. Adv Radiat Oncol 2022;7:100895. https://doi.org/10.1016/j.adro.2022.100895.

[8] Boda-Heggemann J, Frauenfeld A, Weiss C, Simeonova A, Neumaier C, Siebenlist K, et al. Clinical outcome of hypofractionated breath-hold image-guided SABR of primary lung tumors and lung metastases. Radiat Oncol 2014;9:10. https://doi.org/10.1186/1748-717X-9-10.

[9] Scotti V, Marrazzo L, Saieva C, Agresti B, Meattini I, Desideri I, et al. Impact of a breathing-control system on target margins and normal-tissue sparing in the treatment of lung cancer: experience at the radiotherapy unit of Florence University. Radiol Med 2014;119:13–9. https://doi.org/10.1007/s11547-013-0307-6.

[10] Kimura T, Hirokawa Y, Murakami Y, Tsujimura M, Nakashima T, Ohno Y, et al. Reproducibility of organ position using voluntary breath-hold method with spirometer for extracranial stereotactic radiotherapy. Int J Radiat Oncol Biol Phys 2004;60:1307–13. https://doi.org/10.1016/j.ijrobp.2004.07.718.

[11] Ueda Y, Takakura T, Ota S, Kito S, Sasaki K, Shimizu H, et al. Questionnaire survey on treatment planning techniques for lung stereotactic body radiotherapy in Japan. J Radiat Res 2020;61:104–16. https://doi.org/10.1093/jrr/rrz081.

[12] Kamima T, Iino M, Sakai R, Ito Y, Sakae T, Moriya S, et al. Evaluation of the four-dimensional motion of lung tumors during end-exhalation breath-hold conditions using volumetric cine computed tomography images. Radiother Oncol 2023;182:109573. https://doi.org/10.1016/j.radonc.2023.109573.

[13] Rao M, Wu J, Cao D, Wong T, Mehta V, Shepard D, et al. Dosimetric impact of breathing motion in lung stereotactic body radiotherapy treatment using intensity modulated radiotherapy and volumetric modulated arc therapy. Int J Radiat Oncol Biol Phys 2013;87:859. https://doi.org/10.1016/j.ijrobp.2011.12.001.

[14] Huesa-Berral C, Burguete J, Moreno-Jiménez M, Diego AJ. A method using 4D dose accumulation to quantify the interplay effect in lung stereotactic body radiation therapy. Phys Med Biol 2021;66:035025. https://doi.org/10.1088/1361-6560/abd00f.

[15] Shintani T, Nakamura M, Matsuo Y, Miyabe Y, Mukumoto N, Mitsuyoshi T, et al. Investigation of 4D dose in volumetric modulated arc therapy-based stereotactic body radiation therapy: does fractional dose or number of arcs matter? J Radiat Res 2020;61:325–34. https://doi.org/10.1093/jrr/rrz103.

[16] Li X, Yang Y, Li T, Fallon K, Heron DE, Huq MS. Dosimetric effect of respiratory motion on volumetric-modulated arc therapy-based lung SBRT treatment delivered by TrueBeam machine with flattening filter-free beam. J Appl Clin Med Phys 2013;14:4370. https://doi.org/10.1120/jacmp.v14i6.4370.

[17] Azcona JD, Huesa-Berral C, Moreno-Jiménez M, Barbés B, Aristu JJ, Burguete J. A novel concept to include uncertainties in the evaluation of stereotactic body radiation therapy after 4D dose accumulation using deformable image registration. Med Phys 2019;46:4346–55. https://doi.org/10.1002/mp.13759.

[18] Starkschall G, Britton K, McAleer MF, Jeter MD, Kaus MR, Bzdusek K, et al. Potential dosimetric benefits of four-dimensional radiation treatment planning. Int J Radiat Oncol Biol Phys 2009;73:1560–5. https://doi.org/10.1016/j.ijrobp.2008.12.024.

[19] Smolders A, Hengeveld AC, Both S, Wijsman R, Langendijk JA, Weber DC, et al. Inter- and intrafractional 4D dose accumulation for evaluating ΔNTCP robustness in lung cancer. Radiother Oncol 2023;182:109488. https://doi.org/10.1016/j.radonc.2023.109488.

[20] Harris KM, Adams H, Lloyd DC, Harvey DJ. The effect on apparent size of simulated pulmonary nodules of using three standard CT window settings. Clin Radiol 1993;47:241–4.

[21] Miura H, Ozawa S, Doi Y, Nakao M, Kubo K, Kenjo M, et al. Effectiveness of robust optimization in volumetric modulated arc therapy using 6 and 10 MV flattening filter-free beam therapy planning for lung stereotactic body radiation therapy with a breath-hold technique. J Radiat Res 2020;6(61):575–85. https://doi.org/10.1093/jrr/rraa026.

[22] Kimura T, Nagata Y, Eba J, Ozawa S, Ishikura S, Shibata T, et al. A randomized Phase III trial of comparing two dose-fractionations stereotactic body radiotherapy (SBRT) for medically inoperable Stage IA non-small cell lung cancer or small lung lesions clinically diagnosed as primary lung cancer: Japan Clinical Oncology Group Study JCOG1408 (J-SBRT trial). Jpn J Clin Oncol 2017;47:277–81. https://doi.org/10.1093/jjco/hyw198.

[23] Weistrand O, Svensson S. The ANACONDA algorithm for deformable image registration in radiotherapy. Med Phys 2015;42:40–53. https://doi.org/10.1118/1.4894702.

[24] Motegi K, Tachibana H, Motegi A, Hotta K, Baba H, Akimoto T. Usefulness of hybrid deformable image registration algorithms in prostate radiation therapy. J Appl Clin Med Phys 2019;20:229–36. https://doi.org/10.1002/acm2.12515.

[25] Brock KK, Mutic S, McNutt TR, Li H, Kessler ML. Use of image registration and fusion algorithms and techniques in radiotherapy: report of the AAPM Radiation Therapy Committee Task Group No. 132. Med Phys 2017;44:e43-76. doi: 10.1002/mp.12256.

[26] Jaruthien T, Kitpanit S, Kannarunimit D, Nantavithya C, Prayongrat A, Alisanant P, et al. Flattening filter free stereotactic body radiation therapy for lung tumors: outcomes and predictive factors. Transl Cancer Res 2021;10:571–80. https://doi.org/10.21037/tcr-20-3174.

[27] Baumann R, Chan MKH, Pyschny F, Stera S, Malzkuhn B, Wurster S, et al. Clinical Results of Mean GTV Dose Optimized Robotic-Guided Stereotactic Body Radiation Therapy for Lung Tumors. Front Oncol 2018;8:171. https://doi.org/10.3389/fonc.2018.00171.

[28] de Jong EEC, Guckenberger M, Andratschke N, Dieckmann K, Hoogeman MS, Milder M, et al. Variation in current prescription practice of stereotactic body radiotherapy for peripherally located early stage non-small cell lung cancer: Recommendations for prescribing and recording according to the ACROP guideline and ICRU report 91. Radiother Oncol 2020;142:217–23. https://doi.org/10.1016/j.radonc.2019.11.001.

[29] Liang X, Zheng D, Mamalui-Hunter M, Flampouri S, Hoppe BS, Mendenhall N, et al. ITV-Based Robust Optimization for VMAT Planning of Stereotactic Body Radiation Therapy of Lung Cancer. Pract Radiat Oncol 2019;9:38–48. https://doi.org/10.1016/j.prro.2018.08.005.

[30] Edvardsson A, Nordström F, Ceberg C, Ceberg S. Motion induced interplay effects for VMAT radiotherapy. Phys Med Biol 2018;63(8):085012. https://doi.org/10.1088/1361-6560/aab957.

[31] Ali AM, Greenwood JB, Varasteh M, Esteve S, Jeevanandam P, Göpfert, et al. Analysis of the interplay effect in lung stereotactic ablative radiation therapy based on both breathing motion and plan characteristics. J Radiother Pract 2023;22(e75):1–11. https://doi.org/10.1017/S146039692300033X.

[32] Kubo K, Monzen H, Tamura M, Hirata M, Ishii K, Okada W, et al. Minimizing dose variation from the interplay effect in stereotactic radiation therapy using volumetric modulated arc therapy for lung cancer. J Appl Clin Med Phys 2018;19:121–7. https://doi.org/10.1002/acm2.12264.

[33] Stambaugh C, Nelms BE, Dilling T, Stevens C, Latifi K, Zhang G, et al. Experimentally studied dynamic dose interplay does not meaningfully affect target dose in VMAT SBRT lung treatments. Med Phys 2013;40:091710. https://doi.org/10.1118/1.4818255.

[34] Moreno AC, Fellman B, Hobbs BP, Liao Z, Gomez DR, Chen A, et al. Biologically effective dose in stereotactic body radiotherapy and survival for patients with early-stage NSCLC. J Thorac Oncol 2020;15:101–9. https://doi.org/10.1016/j.jtho.2019.08.2505.